ZEBRAFISH
Volume 14, Number 4, 2017

DOI: 10.1089/zeb.2016.1398

A Zebrafish Model of Human Fibrodysplasia Ossificans Progressiva

Melissa LaBonty,[1,2] Nicholas Pray,[2] and Pamela C. Yelick[1,2]

Abstract

Fibrodysplasia ossificans progressiva (FOP) is a rare, autosomal dominant genetic disorder in humans characterized by explosive inflammatory response to injury leading to gradual ossification within fibrous tissues, including skeletal muscle, tendons, and ligaments. A variety of animal models are needed to study and understand the etiology of human FOP. To address this need, here we present characterizations of the first adult zebrafish model for FOP. In humans, activating mutations in the Type I BMP/TGFβ family member receptor, *ACVR1*, are associated with FOP. Zebrafish *acvr1l*, previously known as *alk8*, is the functional ortholog of human *ACVR1*, and has been studied extensively in the developing zebrafish embryo, where it plays a role in early dorsoventral patterning. Constitutively active and dominant negative mutations in zebrafish *acvr1l* cause early lethal defects. Therefore, to study roles for activating *acvr1l* mutations in adult zebrafish, we created transgenic animals expressing mCherry-tagged, heat-shock-inducible constitutively active Acvr1l, Acvr1l^{Q204D}, to investigate phenotypes in juvenile and adult zebrafish. Our studies showed that adult zebrafish expressing heat-shock-induced Acvr1l^{Q204D} develop a number of human FOP-like phenotypes, including heterotopic ossification lesions, spinal lordosis, vertebral fusions, and malformed pelvic fins. Together, these results suggest that transgenic zebrafish expressing heat-shock-inducible Acvr1l^{Q204D} can serve as a model for human FOP.

Keywords: FOP, heterotopic ossification, adult zebrafish disease model

Introduction

HETEROTOPIC OSSIFICATION (HO) is a condition in which bone forms outside of the normal skeleton.[1] Fibrodysplasia ossificans progressiva (FOP), a predominantly sporadic (noninherited) disease that can also be inherited in an autosomal dominant fashion, is characterized by progressive HO.[2–6] Initial diagnosis is usually made based on the presence of big toe malformation identifiable at birth, and later in life through the formation of subsequent joint and vertebral fusions, and HO formation within fibrous tissues, including skeletal muscle, ligaments, and tendons.[5] Notably, the diaphragm, tongue, and cardiac and smooth muscle are unaffected by FOP.[5] FOP patients usually form HO by 7 years of age, experience progressively limited mobility into their teens as the fibrous tissues of their upper body ossify, and are wheel chair bound in their 30s. The median age of survival is 40 years.[5] FOP affects $\sim$1 in every 2 million individuals, and is most commonly acquired by spontaneous germline mutation. All individuals with FOP carry activating mutations in the gene encoding ACVR1 (also known as ALK2), with a majority of cases displaying the classic p.R206H mutation.[7,8]

ACVR1 is a member of the Type I TGFβ/BMP receptor family. In TGFβ/BMP signaling, a common mechanism of signal transduction is utilized, whereby an extracellular ligand dimer, including bone morphogenetic proteins (BMPs), activin, inhibin, and others, initially binds to a Type II receptor dimer.[9] This complex then recruits a Type I receptor dimer, forming a heteromeric complex composed of ligand dimer, Type II receptor dimer, and Type I receptor dimer. Within this complex, the Type II receptors transphosphorylate the Type I receptors in their glycine-serine domains, thereby activating the signaling complex. Activated Type I receptors are then competent to phosphorylate downstream cytoplasmic Smad signaling partners, which subsequently translocate to the nucleus, where they act as transcription factor complexes, in association with other coactivators and corepressors.[9] TGFβ/BMP signaling pathways are

[1]Program in Cell, Molecular, and Developmental Biology, Sackler School of Graduate Biomedical Sciences, Tufts University School of Medicine, Boston, Massachusetts.
[2]Division of Craniofacial and Molecular Genetics, Department of Orthodontics, Tufts University School of Dental Medicine, Boston, Massachusetts.

highly regulated and orchestrate a wide range of cellular processes. In particular, BMP ligands have the unique ability to activate endochondral ossification, a natural pathway for bone formation that is aberrantly activated in HO development in FOP.[10]

The first isolation and characterization of *acvr1l/alk8*, the zebrafish ortholog of human *ACVR1*, were conducted in the Yelick laboratory.[11] In addition to strong sequence homology (84% in serine/threonine kinase domain),[11] zebrafish *acvr1l* maps to a chromosomal region of zebrafish linkage group 2 (LG02) that exhibits significant synteny to human *ACVR1* located on human chromosome 2.[12] The *acvr1l* gene is widely expressed during embryonic development and is also expressed maternally.[11,13] Functional characterization of *acvr1l* during early embryonic development in zebrafish revealed critical roles in early dorsoventral patterning. Single cell injections of constitutively active *acvr1l* mRNA produced ventralized embryos that display expanded ventral structures, including ventral tail mesoderm.[12–14] In contrast, single cell injections of kinase mutated and dominant negative *acvr1l* mRNA resulted in dorsalized embryos exhibiting loss of ventral tissues and shortened tails.[12,13] Expression of either constitutively active or kinase mutated *acvr1l* results in embryonic lethality by $\sim$3 days postfertilization (dpf).[12–14]

To study roles for Acvr1l in later developmental events such as skeletogenesis, we created transgenic zebrafish expressing an mCherry-tagged, heat-shock-inducible copy of Acvr1l containing a Q204D activating mutation, herein called Acvr1l^{Q204D}. The use of a heat-shock-inducible gene expression system allows us to express Acvr1l^{Q204D} after early embryonic dorsoventral patterning has occurred, to study FOP-like disease progression in zebrafish. We also established an effective, automated heat-shock system, based on a previously published design,[15] for both short-term (<1 month) and long-term (>1 month) heat-shock-induced gene expression in juvenile and adult zebrafish. Our experiments using the automated heat-shock system represent the first long-term heat-shock experiments ever used to study an adult zebrafish disease model.

We first demonstrated that heat-shock of transgenic *Tg(acvr1l_Q204D)* embryos at 5 h postfertilization (hpf) induced ubiquitous expression of Acvr1^{Q204D} and resulted in ventralized phenotypes, consistent with previous reports.[12–14] Expression of mCherry-tagged Acvr1l^{Q204D} was confirmed in heat-shocked adults by fluorescence imaging, Western blot analysis, and Acvr1l immunohistochemical (IMC) analysis. We then characterized the development of FOP-like phenotypes in heat-shocked adult *Tg(acvr1l_Q204D)* zebrafish, which included small HO lesions, abnormal spinal curvature, vertebral fusions, and pelvic fin malformations, suggesting that these animals can be used as a model for human FOP. Here we describe our novel methodology for developing and characterizing a heat-shock-inducible adult zebrafish disease model and present our results to date. We describe future studies to enhance the utility of this zebrafish disease model to significantly improve our knowledge and understanding of the cellular and molecular nature of human FOP.

Materials and Methods

Zebrafish husbandry

Zebrafish (*Danio rerio)* were raised in the Tufts Yelick Lab Zebrafish Facility at 28.5°C in a controlled, automated recirculating environment, with 14/10 h light/dark cycle, as previously described.[16] Zebrafish of both sexes were used in this study, at ages indicated in the article. We used the following mutant and transgenic strains: *Tg(Bre:GFP),*[17] *Tg(Bre:*GFP*); Tg(hsp70l:acvr1l-mCherry)* and *Tg(Bre:* GFP*); Tg(hsp70l:acvr1l_Q204D-mCherry).*

Ethics statement

All experimental procedures on zebrafish embryos and larvae were approved by the Tufts University Institutional Animal Care and Use Committee (IACUC) and Ethics Committee.

Generation of transgenic animals

Tg(hsp70l:acvr1l-mCherry) and *Tg(hsp70l:acvr1l_Q204D-mCherry)* constructs were generated using the Tol2kit, a gateway-based cloning kit for generating Tol2 transgenesis plasmids.[18] In brief, the coding sequence for wild type (WT) zebrafish Acvr1l or Acvr1l carrying the activating mutation Q204>D (CAG>GAC) was inserted into the multiple cloning site of pME-MCS, generating pME-*acvr1l* or pME-*acvr1l_Q204D*, respectively. Three-part Gateway cloning recombination reactions were used to combine the p5E-*hsp70l* (1.5 kb hsp70l promoter), one of the two pME constructs, and p3E-mCherrypA (mCherry for C-terminal fusions, plus SV40 late polyA). The combined constructs, *hsp70l:acvr1l-mCherry* and *hsp70l:acvr1l_Q204D-mCherry*, were each inserted into pDestTol2pA2 (an attR4-R3 gate flanked by Tol2 inverted repeats).

*Tg(Bre:*GFP*); Tg(hsp70l:acvr1l-mCherry)* and *Tg(Bre:* GFP*); Tg(hsp70l:acvr1l_Q204D-mCherry)* zebrafish lines were created by single cell injections of the mentioned pDestTol2pA2 constructs and Tol2 transposase mRNA at a final combined concentration of 25 ng/μL in 0.2 M KCl, as previously described[19] into homozygous *Tg(Bre:*GFP*)* embryos. Injected animals were raised to adulthood and incrossed to establish stable homozygous transgenic lines for each construct. The following shorthand names are used in this article: *Tg(hsp70l:acvr1l-mCherry)* is referred to as *Tg(acvr1l)*, protein product as Acvr1l^{WT}; *Tg(hsp70l:acvr1l_Q204D-mCherry)* is referred to as *Tg(acvr1l_Q204D)*, protein product as Acvr1l^{Q204D}.

Heat-shock procedures

To validate the expression and function of Acvr1l^{WT} and Acvr1l^{Q204D}, embryonic zebrafish were heat-shocked for 1 h starting at 5 hpf. In brief, embryos were collected into Eppendorf tubes containing egg water, placed into a beaker containing room temperature (RT) water, and then placed into a 38°C water bath for 1 h. The temperature of the water in the beaker was monitored until it reached 38°C, and heat-shock was allowed to proceed for 1 h, after which the beaker containing the embryos was moved back to RT. After recovery at 28.5°C for 19 h, 24 hpf animals were anesthetized using 150 mg/L tricaine methanesulfonate (Argent Aquaculture, Redmond, WA) and analyzed for fluorescent reporter transgene expression and phenotypic variations.

A long-term automated heat-shock system for juvenile and adult zebrafish was designed as previously described.[15] In brief, submersible heater controller systems (Pro Heat IC 50 W; Won Brothers, Fredericksburg, VA) were calibrated to

heat to 38°C, then placed in individual fish tanks. Each heater was plugged into a power strip, which was connected to an outlet timer (TN111, Intermatic, Spring Grove, IL). Starting at 14 dpf, zebrafish were subjected to a once daily 1-h heat-shock at 38°C. The temperature in each tank was monitored every minute using a four-channel temperature logger with digital display (UX120-006M; Onset Computer, Bourne, MA). At collection time points, animals were lethally anesthetized using 250 mg/L tricaine methanesulfonate and analyzed for reporter transgene expression and phenotypic variations before microcomputed tomography (Micro-CT) analysis, or further processing for histological and/or IHC analyses.

Fluorescence microscopy

Anesthetized embryonic and adult *Tg(Bre:GFP)*, *Tg(Bre:GFP); Tg(acvr1l-mCherry)* and *Tg(Bre:GFP); Tg(acvr1l_Q204D-mCherry)* zebrafish were monitored for mCherry fluorescence using a 10.3 s exposure and for GFP fluorescence using a 4.2 s exposure. All microscope settings were kept constant to allow for comparison of different treatments and transgenic lines. Fluorescence microscopy was conducted using an M2-Bio fluorescent dissecting microscope (Zeiss, Oberkochen, Germany). Images were captured using an Axiocam 503 color camera (Zeiss, Oberkochen, Germany) and processed using AxioVision SE64 microscopy software (Zeiss, Oberkochen, Germany).

Western blotting

Protein lysates were prepared from age- and size-matched adult zebrafish after 3 months of continuous heat-shock as follows. Zebrafish were lethally anesthetized using 250 mg/L tricaine methanesulfonate and then submerged in liquid nitrogen for 5 min. Frozen zebrafish were placed in a chilled mortar and homogenized to obtain a fine powder. The dry powder was then transferred to protein extraction buffer (1:10 volume of powder to extraction buffer)[20] containing protease inhibitors (cOmplete Protease Inhibitor Cocktail, Roche, Indianapolis, IN) and incubated on ice for 10 min. Lysates were clarified by centrifugation at 14,000 *g* for 20 min and stored at −20°C until use. Total protein content was quantified using the DC Protein Assay (Bio-Rad, Hercules, CA). Samples (50 μg) were separated by sodium dodecyl sulphate-polyacrylamide gel electrophoresis (SDS-PAGE) using 12% resolving and 6% stacking gels. Proteins were transferred to polyvinylidene fluoride (PVDF) membranes and blocked for 1 h in 5% milk powder in Tris-buffered saline with Tween-20 (TBST). Membranes were probed overnight at 4°C with the following primary antibodies in 5% milk powder in TBST: rabbit anti-mCherry at 1:1000 (ab167453; Abcam, Cambridge, MA), rabbit anti-GFP at 1:1000 (ab6556; Abcam, Cambridge, MA), and mouse anti-β-actin at 1:10,000 (A-5441; Sigma-Aldrich, St. Louis, MO). Membranes were incubated for 1 h at RT with one of the following peroxidase-conjugated secondary antibodies in 5% milk powder in TBST: goat antirabbit at 1:2000 (7074; Cell Signaling Technology, Danvers, MA) or goat antimouse at 1:5000 (31430; Thermo Fisher Scientific, Waltham, MA). Protein bands were detected by chemiluminescence (Pierce ECL Western Blotting Substrate; Thermo Fisher Scientific, Waltham, MA). The size and density of the protein bands were quantified using ImageJ software (https://imagej.nih.gov/ij/).

Histology and immunohistochemistry

Lethally anesthetized adult zebrafish were fixed in modified Davidson's fixative for 48 h at RT, then rinsed and stored in phosphate-buffered saline (PBS) at 4°C. For paraffin embedding, samples were immersed for 1 h each in graded ethanol (25% and 50% in PBS, 75% in water, 100%), followed by xylene immersion overnight. Samples were transferred to molten Paraplast Plus paraffin (McCormick Scientific, St. Louis, MO) and allowed to equilibrate overnight. Samples were embedded in fresh molten paraffin and allowed to solidify at RT. Paraffin blocks were serially sectioned at 7 μm and mounted on SuperFrost Plus charged glass microscope slides (Fisher Scientific, Pittsburgh, PA). For histological analyses, mounted sections were stained with H&E, Safranin O with a Fast Green counter stain, or Hall's and Brunt's Quadruple (HBQ) stain.[21] For Safranin O staining, slides were submerged in 0.02% Fast Green in 0.2% acetic acid for 15 s followed directly by submersion in 1% Safranin O for 30 s. For HBQ staining, samples were stained in the solutions in the following order: Celestine Blue (C7143; Sigma-Aldrich, St. Louis, MO) for 30 s; Mayer's Hematoxylin (MHS16; Sigma-Aldrich, St. Louis, MO) for 1 min; acid alcohol (0.5% glacial acetic acid in 80% ethanol) for 2 min; Alcian Blue (05500, Sigma-Aldrich, St. Louis, MO) for 5 min; 1% phosphomolybdic acid for 5 min; and 0.5% Direct Red (CI 28160, 195251; Sigma-Aldrich, St. Louis, MO) for 4 min.

Paraffin sections were also used for IHC analyses. In brief, sections were deparaffinized in xylene and then rehydrated through graded ethanol. Endogenous peroxidases were blocked by treatment with 3% hydrogen peroxide in methanol. Antigen retrieval was completed in a steamer using sodium citrate buffer, pH 6.0. Sections were blocked in 10% serum, incubated with primary antibody in 2% serum for 1 h at RT, and then incubated with a horseradish peroxidase (HRP)-conjugated secondary antibody in 2% serum for 45 min at RT. Colorimetric signal was developed by incubation of VECTASTAIN Elite ABC reagent (Vector Laboratories, Burlingame, CA), followed by addition of SIGMAFAST DAB reagent (Sigma-Aldrich, St. Louis, MO). Sections were counterstained with Fast Green as already described. After dehydration, slides were mounted using Permount (Fisher Scientific, Pittsburgh, PA) and cover slipped. All stained slides were observed using a Zeiss AxioPhot epifluorescence microscope (Zeiss, Oberkochen, Germany). Images were captured as described previously.

For IHC analyses, the following antibodies were used: 1:2000 rabbit anti-Acvr1l (custom antibody) and 1:500 donkey antirabbit (Jackson ImmunoResearch Laboratories, West Grove, PA).

Microcomputed tomography

Euthanized adult zebrafish were imaged using a Skyscan 1176 high-resolution Micro-CT Scanner (Bruker, Allentown, PA). Animals were immersed in a small volume of PBS on a piece of plastic wrap to keep them moist while providing the least background interference during the imaging process. Scans were completed at 9 μm resolution, every 0.5° over 180°. Reconstructions were completed using NRecon (Bruker, Allentown, PA) and 3D volume renderings were generating using CTVox (Bruker, Allentown, PA). All reconstruction and rendering settings were kept constant between samples to allow for comparison.

Alizarin red staining

Euthanized adult zebrafish were stained for bone mineralization with Alizarin red, as previously described with minor modifications.[22] In brief, pigment was cleared in a 1% hydrogen peroxide in 1% KOH solution for 2 h. Animals were rinsed in distilled water three times, then transferred to 30% saturated sodium tetraborate (borax) solution overnight. Soft tissues were digested by shaking in 1% trypsin, 2% borax solution for 6 h. Animals were rinsed in distilled water three times, then immersed in 10 mg/mL Alizarin red (A3757; Sigma-Aldrich, St. Louis, MO) in 1% KOH overnight. Animals were rinsed once more in distilled water, then transferred through glycerol: 1% KOH series (20:80, 40:60, 70:30) over the course of 3 days. Animals were transferred to 100% glycerol for imaging and long-term storage.

Spinal angle measurements

The angle of upward (kyphotic) or downward (lordotic) curvature of the spine was measured on a sagittal view of each zebrafish imaged by Micro-CT. In brief, the angle tool on ImageJ was used to place three points: the first at the peak of the curvature of the spine, the second at the Weberian apparatus anterior to the vertebrae, and the third at the hypural joint posterior to the vertebrae. The angle created by these three points was measured and recorded as the spinal angle, in degrees. Positive numbers indicate kyphosis, which is the natural curvature for anterior vertebrae,[23] whereas negative numbers indicate lordosis, which is abnormal spinal curvature in a zebrafish.

Methodology and statistics

All animals established on a given heat-shock system were included in analyses described hereunder. Animal numbers and replicates are indicated in figure legends. Only animals that died of natural causes before desired collection time point were excluded from analyses. Spinal angle measurements were compared with an unpaired *t*-test using GraphPad Prism statistical software.

Results

Generation of Tg(acvr1l_Q204D) *zebrafish for conditional expression of constitutively active Acvr1l*

Before the identification of constitutively activating mutations in *ACVR1* as the underlying cause of FOP in humans,[24] the zebrafish homolog of human *ACVR1*, presently known as *acvr1l* and previously known as *alk8*, was studied for its role in early embryonic development and dorsoventral patterning.[11–14,25] Expression of constitutively active Acvr1l in zebrafish embryos causes ventralization phenotypes, resulting in reduced dorsal neural tissue formation and expanded ventral mesodermal tissue formation.[12–14] These strong phenotypes resulted in early embryonic lethality, prohibiting studies of constitutively active Acvr1l in adult zebrafish development.

Therefore, to study the effects of constitutively activated Acvr1l expression in juvenile and adult zebrafish, we turned to a conditional gene expression system. We used gateway-based cloning to generate constructs containing the coding sequence for WT zebrafish Acvr1l and the Yelick Lab-generated constitutively active Acvr1 (Q204D) mutant (Fig. 1A, B), each driven by the Hsp70 promoter. In addition, each construct contained a C-terminal in-frame mCherry sequence tag to generate a fluorescent Acvr1l-mCherry fusion protein product (Fig. 1C). These constructs were injected into single-cell stage zebrafish embryos along with Tol2 transposase to promote transgene integration. Stable transgenic lines were established for *Tg(hsp70l:acvr1l-mCherry)*, herein called *Tg(acvr1l)*, and *Tg(hsp70l:acvr1l_Q204D-mCherry)*, called *Tg(acvr1l_Q204D)*, which only express the transgenes when exposed to 38°C, and thus exhibit normal embryonic development and patterning when raised at

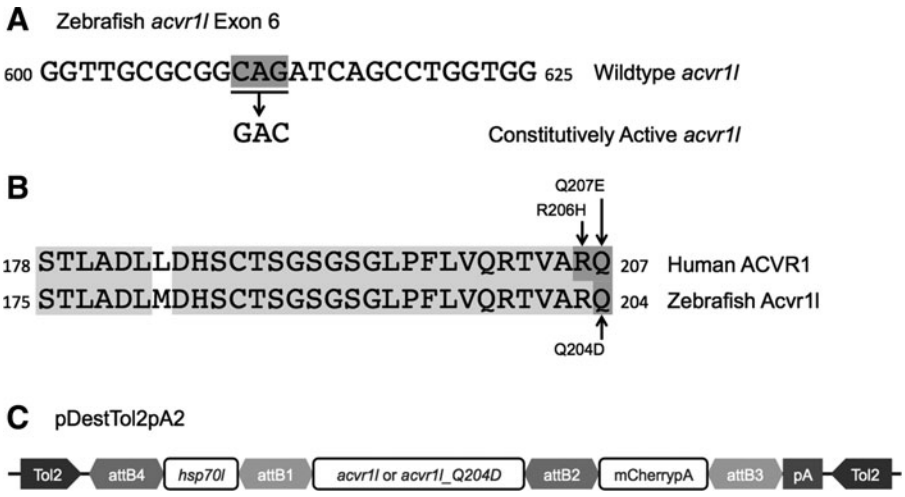

FIG. 1. Generation of *Tg(Bre:GFP); Tg(acvr1l_Q204D-mCherry)* animals. A Yelick laboratory-created construct for constitutively active zebrafish *acvr1l* contains 2 bp mutations converting a CAG to GAC in exon 4 **(A)**. These mutations result in an amino acid change of glutamine (Q) 204 to aspartic acid (D) in the GS domain of the zebrafish Acvr1l protein **(B)**. Zebrafish Acvr1l p.Q204D is homologous to human ACVR1 p.Q207D, which is one of the variants (along with p.R206H) in the GS domain commonly mutated in FOP patients. **(C)** Schematic of pDestTol2pA2 constructs to generate *Tg(hsp70l:acvr1l-mCherry)* and *Tg(hsp70l:acvr1l_Q204D-mCherry)*. FOP, fibrodysplasia ossificans progressiva; GS, glycine-serine.

28.5°C. We injected each of the heat-shock constructs into the transgenic *Tg(Bre:GFP)* zebrafish line, which carries a reporter construct containing five tandem BMP response elements driving GFP expression.[17] This reporter line allows us to directly assess the level of activation of BMP signaling in *Tg(acvr1l)* or *Tg(acvr1l_Q204D)* transgenic zebrafish using GFP fluorescent microscopy.

Automated heat-shock system delivers reliable short-term and long-term heat-shock

Heat-shock induction of gene expression is a well-established method in zebrafish for studying the spatial and temporal roles of proteins *in vivo*.[26] However, few studies have applied heat-shock technology for long-term (>1 month) expression studies in juvenile and adult zebrafish and none have used this technology to generate adult zebrafish disease models. Recently, an economical heat-shock system was established that can be added to any existing re-circulating zebrafish rack, which allows for automation of the heat-shock temperature, duration, and frequency.[15] We have outfitted our zebrafish facility with three independent heat-shock systems (Fig. 2A), each of which is equipped with a temperature logger that registers the temperature in each of up to four tanks, every minute (Fig. 2B). The data from the temperature loggers can be downloaded to a laboratory computer and graphed to display heat-shock regimens over time (Fig. 2C).

When establishing our FOP zebrafish heat-shock model, we found the greatest long-term survival using zebrafish that were at least 14 dpf at the start of a heat-shock experiment. We found that daily heat-shock of animals at 7 dpf resulted in the loss of greater than 50% of animals by 14 dpf. Consistent with previous findings,[15] we found that a low flow rate of 10–20 mL/min was ideal for reaching and maintaining peak heat-shock temperatures. We determined by fluorescence imaging (mCherry) that once daily heat-shock for 1 h is sufficient to induce and maintain continuous Acvr1l^{WT} or Acvr1l^{Q207D}-mCherry protein expression. To date, we have used our heat-shock systems to effectively run experiments ranging in duration from 1 week to 1 year of daily heat-shock on a single cohort of animals.

Functional heat-shock Tg(acvr1l_Q204D-mCherry) *constructs are expressed in embryonic and adult stage zebrafish*

To confirm the expression of Acvr1l^{Q207D}-mCherry in the *Tg(Bre:GFP)* reporter background, we first examined expression in embryonic zebrafish. In brief, 5 hpf embryos were treated with 1 h of heat-shock, and then were analyzed under fluorescent microscopy for mCherry and GFP expression, and using bright field microscopy to confirm the previously characterized ventralized phenotype caused by upregulated BMP signaling.[12–14] Heat-shocked *Tg(Bre:GFP)* zebrafish exhibited GFP expression in tissues in which BMP signaling

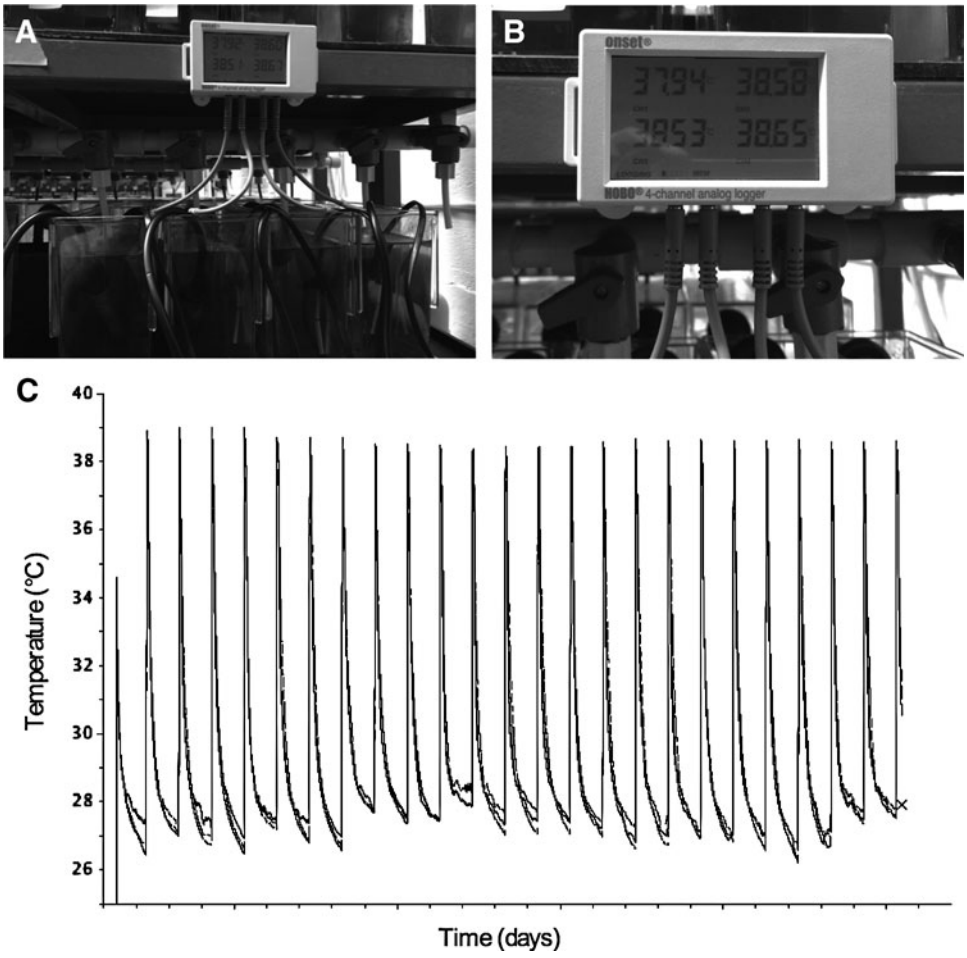

FIG. 2. Establishment of automated heat-shock system for long-term experiments. Automated heat-shock systems established by installing individual tank heaters in system tanks **(A)**. Heaters were calibrated to perform a once daily 1-h heat-shock at 38°C, which was monitored every minute of every day by a temperature logger **(B, C)**.

is normally active at 24 hpf, including the eye and the somites (Fig. 3C),[17] but exhibited no mCherry expression at 24 hpf (only yolk autofluorescence is visible) (Fig. 3B). Dorsoventral patterning appeared normal in *Tg(Bre:GFP)* expressing animals (Fig. 3A). Heat-shocked zebrafish carrying both *Tg(Bre:GFP)* and *Tg(acvr1l-mCherry)* transgenes also exhibited normal dorsoventral patterning (Fig. 3D) and displayed normal GFP expression patterns (Fig. 3F). mCherry was ubiquitously expressed in these animals, as expected for an *hsp70l*-induced transgene (Fig. 3E). The expression of Acvr1l^{WT}-mCherry after heat-shock did not confer any phenotypic abnormalities and animals proceeded through embryonic development normally, as previously reported.[12] In contrast, heat-shocked zebrafish expressing *Tg(acvr1l_Q204D-mCherry)* in the *Tg(Bre:GFP)* background exhibited consistent ventralized phenotypes (Fig. 3G). mCherry fluorescence was ubiquitous in these animals indicating widespread expression of Acvr1l^{Q204D} (Fig. 3H), and upregulated GFP expression was observed in nearly all tissues of these animals (Fig. 3I), indicative of upregulated BMP signaling.[27,28]

Once confirmed in the embryo, we next investigated functional expression of Acvr1l^{Q204D}-mCherry;*Tg(Bre:GFP)* in adult zebrafish, using fluorescence imaging, Western blotting, and IHC analysis of transgenic animals after 3 months of daily heat-shock (Figs. 4 and 5). At 3 months, adult heat-shocked *Tg(Bre:GFP)* zebrafish exhibited GFP expression most prominently in the lens of the eye; although ubiquitous GFP expression throughout the body was detectable anywhere, pigment was absent (Fig. 4C). mCherry expression was not detected in these animals (Fig. 4B). In contrast, adult heat-shocked *Tg(Bre:GFP); Tg(acvr1l_Q204D-mCherry)* zebrafish exhibited mCherry expression throughout the animal, including very bright expression in the lens of the eye (Fig. 4E). These animals also exhibited ubiquitous GFP expression; however, this expression did not appear significantly brighter than heat-shocked *Tg(Bre:GFP)* adults (Fig. 4F), suggesting that visual quantification of GFP fluorescence in live adult zebrafish is likely obscured by the size, scales, and pigmentation of adult zebrafish. Therefore, to confirm that heat-shocked adult *Tg(Bre:GFP); Tg(acvr1l_Q204D-mCherry)* zebrafish exhibited upregulated BMP signaling in response to the expression of Acvr1l^{Q204D}, we used Western blotting to quantify mCherry and GFP protein levels in whole animal protein lysates (Fig. 4G). These analyses showed that only *Tg(Bre:GFP); Tg(acvr1l_Q204D-mCherry)* zebrafish expressed mCherry, with a band at 84 kDa indicative of the Acvr1l-mCherry fusion protein, as expected. We also observed a second band at 27 kDa indicative of free mCherry, suggesting some level of instability and cleavage of the Acvr1l-mCherry fusion protein. We found that heat-shocked *Tg(Bre:GFP); Tg(acvr1l_Q204D-mCherry)* zebrafish exhibited a 3.2-fold increase in GFP protein expression as compared with heat-shocked *Tg(Bre:GFP)* zebrafish, indicative of upregulated BMP signaling in animals expressing constitutively active Acvr1l. Together, these results demonstrate that heat-shock-induced Acvr1l^{Q204D}-mCherry is functional in adult and embryonic zebrafish, and is capable of inducing upregulated BMP signaling measured by increased GFP protein expression.

In addition to validating heat-shock-induced Acvr1l^{Q204D}-mCherry expression by fluorescence imaging and Western blotting, Acvr1l^{Q204D}-mCherry expression was also validated

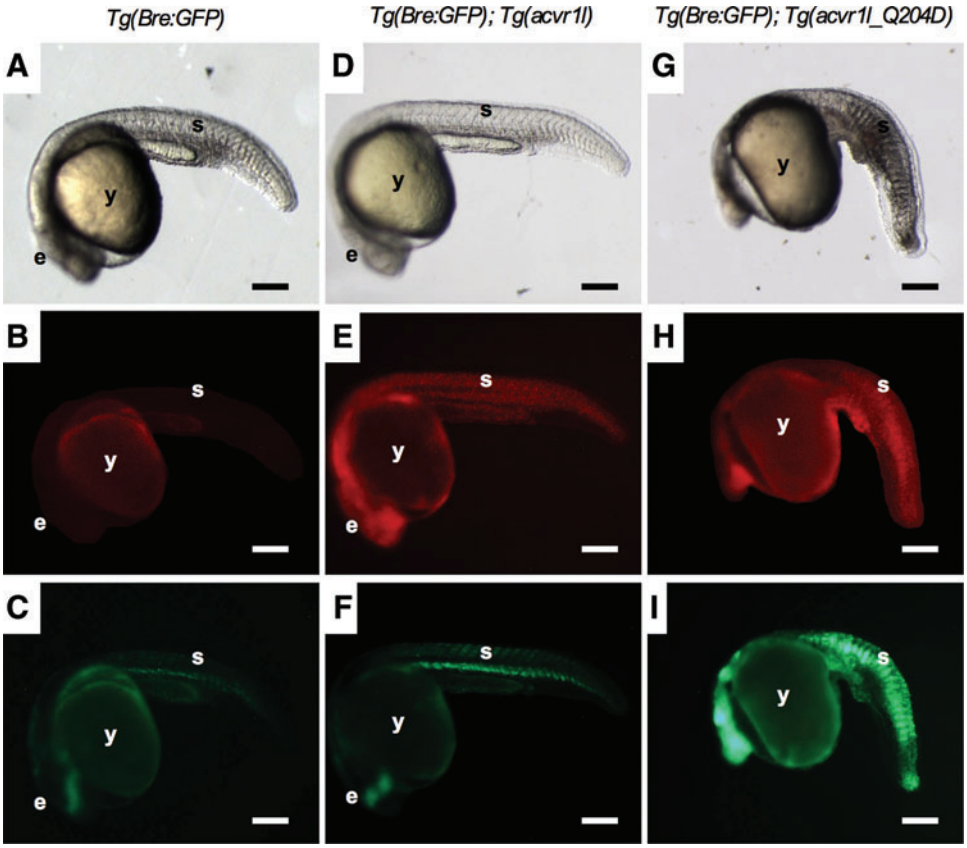

FIG. 3. *Tg(Bre:GFP); Tg(acvr1l_Q204D-mCherry)* embryos exhibit ventralized phenotypes and increased *Tg(Bre:GFP)* reporter expression. *Tg(Bre:GFP)* **(A–C)**, *Tg(Bre:GFP); Tg(acvr1l-mCherry)* **(D–F)**, and *Tg(Bre:GFP); Tg(acvr1l_Q204D-mCherry)* **(G–I)** embryos at 24 hpf, after 1 h of heat-shock at 5 hpf. Embryos were analyzed through fluorescent microscopy for mCherry **(B, E, H)** and GFP **(C, F, I)** fluorescence intensity, and through bright field microscopy for gross morphological phenotypes **(A, D, G)**. $n = 10$ embryos each, for at least three replicate experiments. Scale bar is 200 μm. e, eye; GFP, green fluorescent protein; hpf, hour postfertilization; s, somites; y, yolk. Color images available online at www.liebertpub.com/zeb

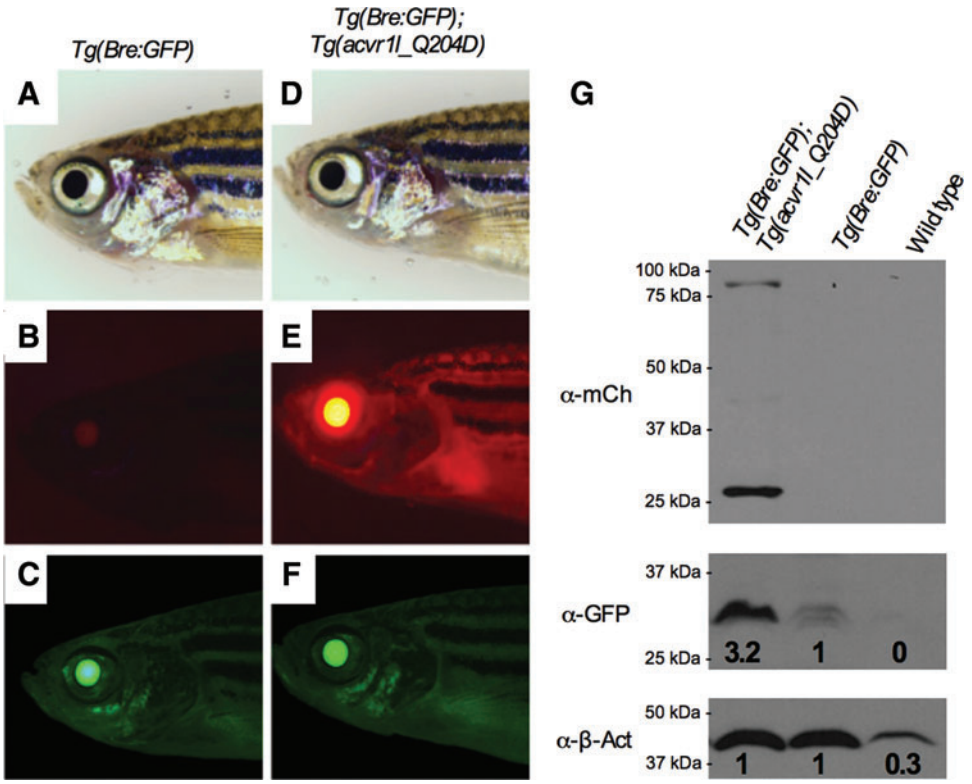

FIG. 4. Acvr1l^{Q204D} is expressed in heat-shocked adult zebrafish. After 3 months of once daily heat-shock for 1 h at 38°C, adult *Tg(Bre:GFP)* **(A–C)** and *Tg(Bre:GFP); Tg(acvr1l_Q204D-mCherry)* **(D–F)** zebrafish were characterized through bright field microscopy **(A, D)** and through fluorescent microscopy for mCherry **(B, E)** and GFP **(C, F)** fluorescence intensity ($n=5$ adult zebrafish). **(G)** Western blots of protein extracts from the same animals were probed using anti-mCherry (Acvr1l-mCherry at 84 kDa and free mCherry at 27 kDa), anti-GFP (27 kDa), and anti-β-actin (43 kDa) antibodies ($n=2$ replicate Western blots). Color images available online at www.liebertpub.com/zeb

using paraffin section IHC for Acvr1l (Fig. 5). Endogenous levels of Acvr1l were detected in heat-shocked *Tg(Bre:GFP)* zebrafish in most tissues, including the intestines (Fig. 5B) and the muscle tissue (Fig. 5E, H); however, it was absent from the liver (Fig. 5B). Upregulated and ubiquitous Acvr1l expression was detected in heat-shocked *Tg(Bre:GFP); Tg(acvr1l_Q204D)* zebrafish, as seen in the intestines, liver, and muscle tissue (Fig. 5C, F, I), consistent with expression of both endogenous Acvr1l and heat-shock-induced Acvr1l^{Q204D} proteins. Previous work from the Yelick laboratory has demonstrated Acvr1l receptor specificity for this antibody.[29] No Acvr1l expression was detected in samples lacking the primary antibody (Fig. 5A, D, G). Together, our fluorescence imaging, Western blot, and IHC results confirmed the expression of functionally active Acvr1l^{Q204D} in both embryonic and adult heat-shocked zebrafish.

Micro-CT analyses of heat-shocked Tg(acvr1l_Q204D) *zebrafish reveal phenotypes indicative of FOP*

After verifying functional expression of Acvr1l^{Q204D} in heat-shocked adult zebrafish, we next sought to determine whether FOP-like phenotypes were evident in these animals. *Tg(Bre:GFP); Tg(acvr1l_Q204D-mCherry)* zebrafish were heat-shocked daily for 3 to 8 months before euthanization and imaging with Micro-CT (Table 1 and Fig. 6). All of the eight heat-shocked *Tg(Bre:GFP); Tg(acvr1l_Q204D-mCherry)* zebrafish examined displayed some degree of spinal lordosis (Fig. 6B, C), in distinct contrast to the slightly kyphotic spinal curvature exhibited by age-matched non-heat-shocked and heat-shocked *Tg(Bre:GFP)* zebrafish (Fig. 6A). The average angle of spinal curvature in the *Tg(Bre:GFP); Tg(acvr1l_Q204D-mCherry)* zebrafish was −3.27°, indicative of downward or lordotic curvature (Fig. 6D). This angle was statistically significantly different from the average angle of the *Tg(Bre:GFP)* zebrafish, 7.74°. Thoracic lordosis is a known developmental phenotype of FOP patients.[5]

In addition to the fully penetrant lordosis phenotype observed in heat-shocked *Tg(Bre:GFP); Tg(acvr1l_Q204D-mCherry)* zebrafish, several other FOP phenotypes were observed in some animals. Significantly, 3/8 animals (37.5%) developed small HO lesions just behind the dorsal fin (Fig. 6H, arrow), and 1/8 animals exhibited significant HO throughout the body cavity (Fig. 6F, arrow). None of the heat-shocked *Tg(Bre:GFP)* zebrafish developed HO within the body cavity (Fig. 6E, G). As previously described, HO is one of the hallmark characteristics of human FOP patients.[3,7] Furthermore, we found 3/8 animals (37.5%) displayed single vertebral fusions (Fig. 6J, arrow), which were never observed in heat-shocked *Tg(Bre:GFP)* control animals (Fig. 6I). Vertebral fusions are a common variable phenotype of human FOP.[5] In addition, 1/8 heat-shocked *Tg(Bre:GFP); Tg(acvr1l_Q204D-mCherry)* animals (12.5%) showed a strong malformation of both pelvic fins (Fig. 6L, N, arrows), easily identified as compared with control *Tg(Bre:GFP)* zebrafish (Fig. 6K, M). Recent work has provided strong support for common developmental pathways driving fish fin ray formation and tetrapod digit formation,[30] suggesting that this partially penetrant phenotype could be reminiscent of the big toe malformation associated with classical human FOP, despite being more severe than the human phenotype.[5,7]

Histological analyses of HO from FOP zebrafish

After successfully identifying HO in heat-shocked *Tg(Bre:GFP); Tg(acvr1l_Q204D)* zebrafish by Micro-CT,

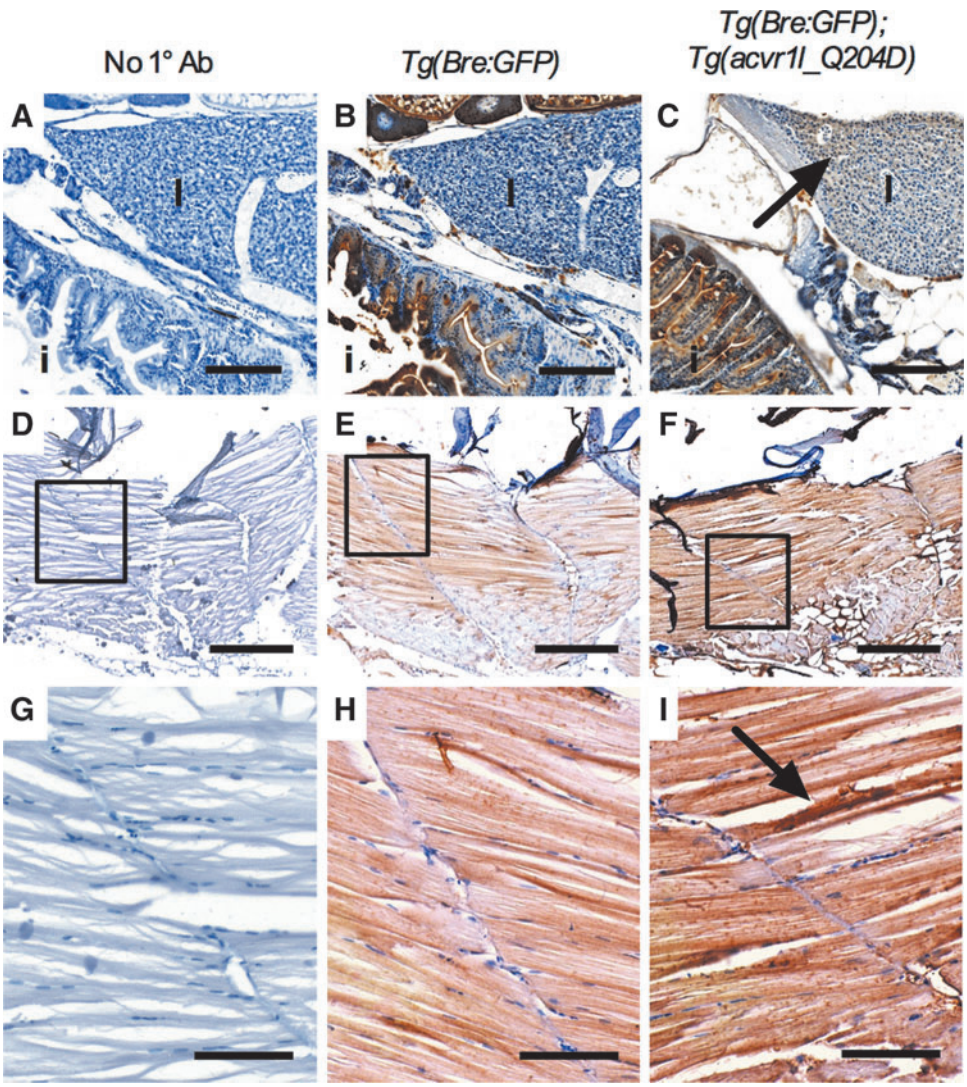

FIG. 5. Acvr1l^{Q204D} protein expression is ubiquitous. Sagittal paraffin sections of imaged adult *Tg(Bre:GFP)* (**B**: 20×, **E**: 10×, **H**: 40×) and *Tg(Bre:GFP); Tg(acvr1l_Q204D-mCherry)* (**C**: 20×, **F**: 10×, **I**: 40×) zebrafish were used to analyze Acvr1l expression by IHC. No primary controls were negative (**A**: 20×, **D**: 10×, **G**: 40×). *Arrows* point to regions of greater Acvr1l expression in *Tg(Bre:GFP); Tg(acvr1l_Q204D-mCherry)* zebrafish **(C, I)**. **(G, H)** are enlarged views of areas indicated by *boxes* in **(D–F)**, respectively. **(A–C)** 20×scale bar is 150 μm. **(D–F)** 10×scale bar is 400 μm. **(G–I)** 40×scale bar is 80 μm. i, intestines; IHC, immunohistochemical; l, liver. Color images available online at www.liebertpub.com/zeb

these lesions were analyzed at the cellular level using histological analyses, including H&E, Safranin O, and HBQ stains.[21] H&E-stained sagittal sections of the heat-shocked *Tg(Bre:GFP); Tg(acvr1l_Q204D)* zebrafish exhibiting HO lesions throughout the body cavity (Table 1, Fish 6; Fig. 6F) revealed numerous mineralized tissue-like masses (Fig. 7A—box, D—arrow). Safranin-O-stained serial sections revealed dark red staining, indicative of cartilaginous proteoglycans (Fig. 7B—box, E—arrow). HBQ-stained serial sections exhibited pink staining, indicative of mineralized tissue formation (Fig. 7C box, F arrow). Positive staining for both cartilaginous proteoglycans and mineralization is a common feature of human HO lesions.[31,32]

TABLE 1. FIBRODYSPLASIA OSSIFICANS PROGRESSIVA-LIKE PHENOTYPES IN TG(ACVR1L_*Q*204*D*-MCHERRY) ZEBRAFISH

	3 Months HS			*8 Months HS*					
	Fish 1 (Male)	*Fish 2 (Female)*	*Fish 3 (Male)*	*Fish 4 (Female)*	*Fish 5 (Male)*	*Fish 6 (Female)*	*Fish 7 (Male)*	*Fish 8 (Male)*	*Total (%)*
Lordosis	Yes	Yes	Yes	Yes	Yes	Yes	Yes	Yes	8/8 (100)
Vertebral fusion	No	Yes	No	No	Yes	No	No	Yes	3/8 (37.5)
HO lesions	No	No	No	No	No	Yes	Yes	Yes	3/8 (37.5)
Malformed pelvic fins	Yes	No	No	No	No	No	No	No	1/8 (12.5)

Tg(Bre:GFP); Tg(acvr1l_Q204D-mCherry) animals analyzed by microcomputed tomography after 3 or 8 months of heat-shock displayed various FOP-like phenotypes.

FOP, fibrodysplasia ossificans progressiva; HO, heterotopic ossification; HS, heat-shock.

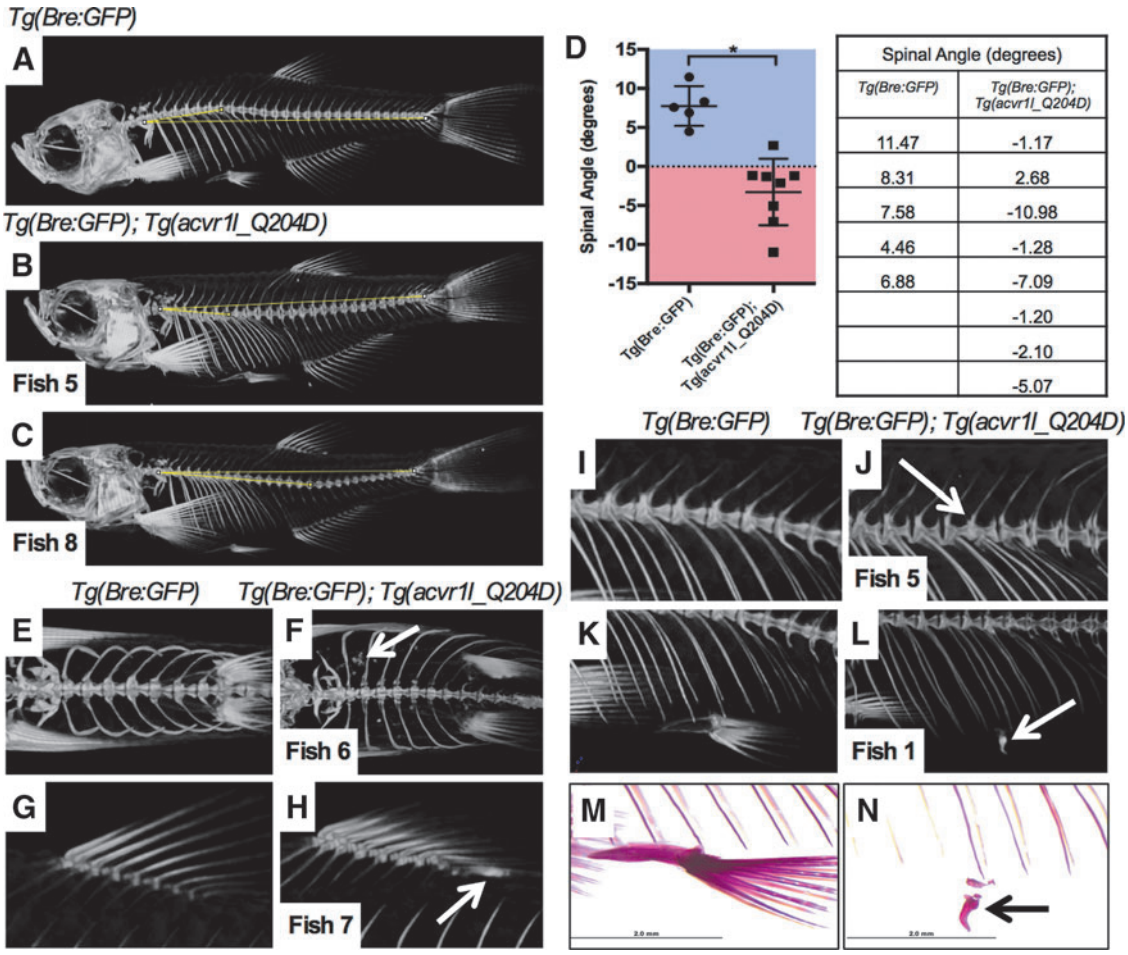

FIG. 6. Expression of Acvr1l^{Q204D} in zebrafish generates FOP-like phenotypes. Microcomputed tomography imaging of zebrafish expressing Acvr1l^{Q204D}-mCherry revealed a variety of FOP-like phenotypes, including spinal lordosis (**B, C,** quantified in **D**) as compared with age-matched *Tg(Bre:GFP)* animals **(A)**; HO (**F**, **H**, *arrows* vs. **E**, **G**); vertebral fusion (**J**, *arrow* vs. **I**); and malformed pelvic fins (**L**, *arrow* vs. **K**). Alizarin red staining of zebrafish harboring malformed pelvic fins indicated abnormal mineralization of structures (**N**, *arrow*). Control *Tg(Bre:GFP)* zebrafish did not exhibit any of these phenotypes **(A, E, G, I, K, M)**. Panels containing zebrafish expressing Acvr1l^{Q204D}-mCherry labeled with fish number corresponding to Table 1. $n=8$ *Tg(Bre:GFP); Tg(acvr1l_Q204D-mCherry)* animals, and $n=5$ *Tg(Bre:GFP)* animals. *Indicates statistical significance of $p<0.001$. HO, heterotopic ossification. Color images available online at www.liebertpub.com/zeb

Discussion

In this study, we describe the creation and characterization of the first heat-shock-inducible adult zebrafish disease model. Adult zebrafish expressing heat-shock-inducible *Tg(acvr1l_Q204D)*, a transgene encoding a constitutively active form of the zebrafish ortholog of the FOP-associated human gene *ACVR1*, developed a variety of FOP-like phenotypes, including HO, fused vertebrae, pelvic fin malformations, and abnormal spinal lordosis. The significant HO that developed in a heat-shocked *Tg(acvr1l_Q204D)* zebrafish strongly resembled that observed in human FOP patients, and in an FOP mouse model that was characterized using Micro-CT and histological analyses.[31,33–35] Although the activating mutation p.Q204D used in these experiments does not naturally occur in human FOP patients, the development of phenotypes associated with FOP suggests that heat-shock-inducible *Tg(acvr1l_Q204D)* zebrafish can still serve as a useful model for studying human FOP.

The variability of penetrance of the phenotypes observed in the heat-shock-inducible *Tg(acvr1l_Q204D)* zebrafish is reminiscent of the variability in the severity of FOP in humans.[5] Only two features of the disease in humans are considered to be fully penetrant and classical hallmarks of the disease: malformation of the big toes and progressive HO formation.[3] Even the rates of HO formation can vary greatly between human patients, with some individuals immobilized by their HO growth by 20 years of age, whereas others remain nearly unaffected in the same time frame. Most other phenotypes associated with FOP are atypical and variable. For example, osteochondromas develop in >90% of patients, cervical spine malformations affect >80% of patients, and thumb malformations affect ~50% of patients.[7] In addition, some FOP patients present with rare, previously undocumented phenotypes, including loss of digits, growth retardation, aplastic anemia, cataracts, and retinal detachment, to name a few.[7] This wide range of variability in the development of human FOP phenotypes

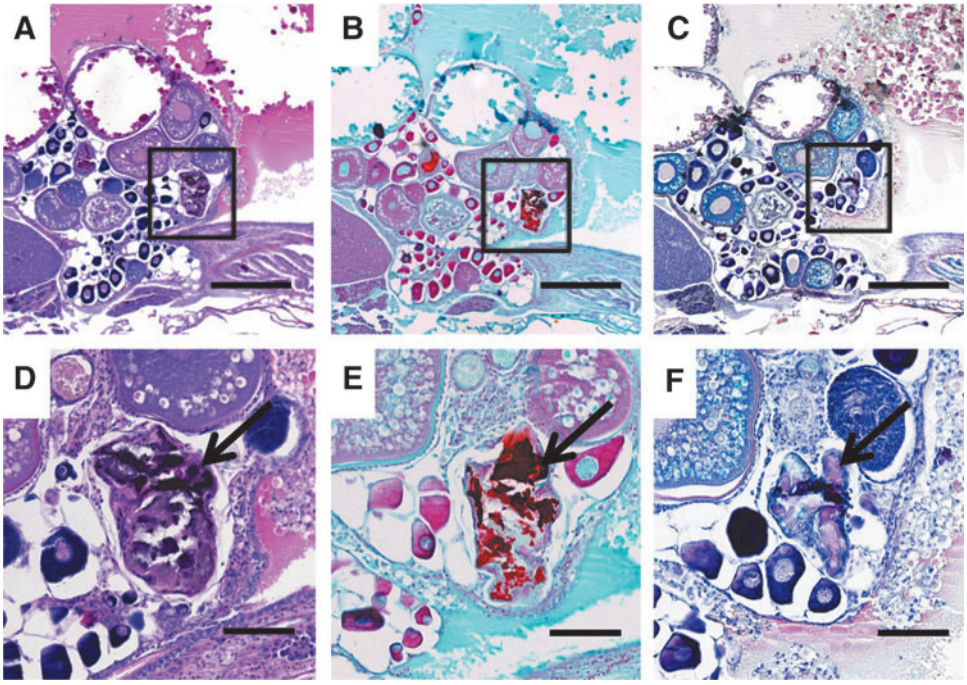

FIG. 7. Histology of HO in *Tg(acvr1l_Q204D-mCherry)* zebrafish. H&E **(A, D)**, Safranin O **(B, E)**, and HBQ **(C, F)**-stained paraffin sectioned *Tg(Bre:GFP); Tg(acvr1l_Q204D-mCherry)* zebrafish **(A–F)**. Sagittal sections of zebrafish exhibiting HO throughout the body cavity revealed numerous proteoglycan-dense (**B**, **E**, strong red Safranin O stain), ossified (**C**, **F**, pinkish-red from HBQ stain) masses adjacent to the ovary (*boxed* in **A–C**, *arrows* in **D–F**). **(D–F)** are enlarged views of areas indicated by *boxes* in **(A–C)**, respectively. **(A–C)** 5× scale bar is 400 μm. **(D–F)** 20× scale bar is 100 μm. HBQ, Hall's and Brunt's Quadruple. Color images available online at www.liebertpub.com/zeb

suggests that the variability seen in the first adult zebrafish model for FOP is to be expected.

These results are particularly exciting because of the numerous advantages afforded by modeling FOP in the zebrafish. First, genetic modifier screens for FOP can be most easily conducted in zebrafish. In human patients with FOP, there is great variability in the severity of phenotypes and in the rate of disease progression.[5] It is likely that this variability is caused, in part, by additional uncharacterized genetic mutations that synergize with constitutively active Acvr1 to either suppress or exacerbate disease progression. Such mutations could be efficiently identified in a zebrafish model for FOP using well-established tools for mutagenesis, such as chemical N-ethyl-nitroso-urea,[36] and screening mutagenized animals for alterations in characterized phenotypes. Second, zebrafish are an ideal model system to quickly validate existing therapeutic compounds identified through *in vitro* cell-based assays. In addition, small molecule screens are readily performed in zebrafish as compared with rodent models, and can be used to identify novel signaling pathways that can potentially be exploited as new therapeutic inroads to treat human FOP. *In vivo* drug screens in animals typically provide superior candidates to *in vitro* cell-based assays and also provide insight into the pharmacological properties of drugs, such as metabolism and toxicity. Of all the model organisms amenable to drug screens—yeast, worms, flies, and zebrafish—only zebrafish possess organ systems with well-conserved physiology to human organs.[37] Third, zebrafish have fully functional innate and adaptive immune systems, which are similar to human immune systems.[38] Functional conservation of these systems is critical, as recent research suggests an integral role for immunological triggers in the progression of FOP.[39]

The majority of heat-shocked *Tg(acvr1l_Q204D)* zebrafish did not spontaneously develop large HO lesions, as was expected. In retrospect, this may not be entirely surprising, because of the fact that in humans, FOP lesion formation is initiated by accidental injuries, which rarely, if ever, occur in a zebrafish facility laboratory setting. Indeed, lack of spontaneous HO formation has been observed in other FOP animal models.[40] In numerous published animal model FOP studies, an injury model was used to induce HO.[31,34,35,40–42] Advantages that could be afforded by introducing an injury model for FOP zebrafish include reproducibility, easy identification of targeted lesion site, and the potential to perform time course analyses of disease progression. Given these findings, we intend to further our studies by incorporating the future design and implementation of an injury model for our heat-shocked *Tg(acvr1l_Q204D)* FOP zebrafish.

In addition to establishing an injury model for heat-shock-inducible *Tg(acvr1l_Q204D)* FOP zebrafish, future studies will use gene editing techniques such as CRISPR-Cas9 to introduce human FOP-associated mutations at the endogenous zebrafish *acvr1l* locus. Two common FOP-associated mutations in human *ACVR1* are p.R206H (p.R203H in zebrafish) and p.Q207E (p.Q204E in zebrafish) (Fig. 1B).[7,8,43] It is yet to be determined whether heterozygous expression of constitutively active zebrafish *acvr1l* under the control of its endogenous promoter will cause embryonic lethality because of ventralization phenotypes, or whether these animals will successfully undergo embryonic development and subsequently acquire FOP-like phenotypes, as observed in human FOP patients. These approaches may provide a more robust zebrafish model of FOP with which to address further questions in the field.

In summary, this study introduces the first zebrafish model resembling human FOP. Given the conservation of organ system development and physiology between humans and zebrafish, this model provides a new and valuable *in vivo* tool for studying FOP. Future studies will exploit the advantages of the zebrafish model to fill gaps in our knowledge and understanding of the genetic and molecular mechanisms driving FOP disease progression.

Acknowledgments

The authors sincerely thank Peter Kovach, Viktoria Andreeva, Nicole Fisher, Sophie Chase, Kei Thurber, Patricia Hare, John Lyons, and Siobhan McRee for expert technical support and helpful discussions. Funding: this work was supported by NIH/NIDCR R01DE018043 (P.C.Y.) and R21AR065761 (P.C.Y.), and NSF GRFP NS9344 (M.L.). The funders had no role in study design, data collection and analysis, decision to publish, or preparation of the article.

Authors' Contribution

M.L. and P.C.Y. conceived and designed the experiments. M.L. and N.P. performed the experiments. M.L., N.P., and P.C.Y. analyzed the data. M.L. and P.C.Y. contributed reagents/materials/analysis tools. M.L. and P.C.Y. wrote the article.

Disclosure Statement

No competing financial interests exist.

References

1. McCarthy EF, Sundaram M. Heterotopic ossification: a review. Skeletal Radiol 2005;34:609–619.
2. Kaplan FS, Tabas JA, Gannon FH, *et al.* The histopathology of fibrodysplasia ossificans progressiva. An endochondral process. J Bone Joint Surg Am 1993;75:220–230.
3. Kaplan FS, Le Merrer M, Glaser DL, *et al.* Fibrodysplasia ossificans progressiva. Best Pract Res Clin Rheumatol 2008;22:191–205.
4. Kartal-Kaess M, Shore EM, Xu M, *et al.* Fibrodysplasia ossificans progressiva (FOP): watch the great toes! Eur J Pediatr 2010;169:1417–1421.
5. Pignolo RJ, Shore EM, Kaplan FS. Fibrodysplasia ossificans progressiva: clinical and genetic aspects. Orphanet J Rare Dis 2011;6:80.
6. Kaplan FS, Chakkalakal SA, Shore EM. Fibrodysplasia ossificans progressiva: mechanisms and models of skeletal metamorphosis. Dis Model Mech 2012;5:756–762.
7. Kaplan FS, Xu M, Seemann P, *et al.* Classic and atypical fibrodysplasia ossificans progressiva (FOP) phenotypes are caused by mutations in the bone morphogenetic protein (BMP) type I receptor ACVR1. Hum Mutat 2009;30:379–390.
8. Hildebrand L, Stange K, Deichsel A, Gossen M, Seemann P. The fibrodysplasia ossificans progressiva (FOP) mutation p.R206H in ACVR1 confers an altered ligand response. Cell Signal 2017;29:23–30.
9. Derynck R, Zhang YE. Smad-dependent and Smad-independent pathways in TGF-beta family signalling. Nature 2003;425:577–584.
10. Shore EM, Kaplan FS. Inherited human diseases of heterotopic bone formation. Nat Rev Rheumatol 2010;6:518–527.
11. Yelick PC, Abduljabbar TS, Stashenko P. zALK-8, a novel type I serine/threonine kinase receptor, is expressed throughout early zebrafish development. Dev Dyn 1998;211:352–361.
12. Payne TL, Postlethwait JH, Yelick PC. Functional characterization and genetic mapping of alk8. Mech Dev 2001;100:275–289.
13. Mintzer KA, Lee MA, Runke G, *et al.* Lost-a-fin encodes a type I BMP receptor, Alk8, acting maternally and zygotically in dorsoventral pattern formation. Development 2001;128:859–869.
14. Bauer H, Lele Z, Rauch GJ, Geisler R, Hammerschmidt M. The type I serine/threonine kinase receptor Alk8/Lost-a-fin is required for Bmp2b/7 signal transduction during dorsoventral patterning of the zebrafish embryo. Development 2001;128:849–858.
15. Duszynski RJ, Topczewski J, LeClair EE. Simple, economical heat-shock devices for zebrafish housing racks. Zebrafish 2011;8:211–219.
16. Westerfield M. The Zebrafish Book. A Guide for Laboratory Use of Zebrafish (*Danio rerio*), University of Oregon Press, Eugene, 1995.
17. Alexander C, Zuniga E, Blitz IL, *et al.* Combinatorial roles for BMPs and Endothelin 1 in patterning the dorsal-ventral axis of the craniofacial skeleton. Development 2011;138:5135–5146.
18. Kwan KM, Fujimoto E, Grabher C, *et al.* The Tol2kit: a multisite gateway-based construction kit for Tol2 transposon transgenesis constructs. Dev Dyn 2007;236:3088–3099.
19. Kawakami K. Transgenesis and gene trap methods in zebrafish by using the Tol2 transposable element. Methods Cell Biol 2004;77:201–222.
20. Braun MH, Steele SL, Perry SF. The responses of zebrafish (*Danio rerio*) to high external ammonia and urea transporter inhibition: nitrogen excretion and expression of rhesus glycoproteins and urea transporter proteins. J Exp Biol 2009;212(Pt 23):3846–3856.
21. Hall BK. The role of movement and tissue interactions in the development and growth of bone and secondary cartilage in the clavicle of the embryonic chick. J Embryol Exp Morphol 1986;93:133–152.
22. Connolly MH, Yelick PC. High-throughput methods for visualizing the teleost skeleton: capturing autofluorescence of alizarin red. J Appl Ichthyol 2010;26:274–277.
23. Boswell CW, Ciruna B. Understanding idiopathic scoliosis: A new zebrafish school of thought. Trends Genet 2017;33:183–196.
24. Shore EM, Xu M, Feldman GJ, *et al.* A recurrent mutation in the BMP type I receptor ACVR1 causes inherited and sporadic fibrodysplasia ossificans progressiva. Nat Genet 2006;38:525–527.
25. Tucker JA, Mintzer KA, Mullins MC. The BMP signaling gradient patterns dorsoventral tissues in a temporally progressive manner along the anteroposterior axis. Dev Cell 2008;14:108–119.
26. Shoji W, Sato-Maeda M. Application of heat shock promoter in transgenic zebrafish. Dev Growth Differ 2008;50:401–406.
27. Hammerschmidt M, Serbedzija GN, McMahon AP. Genetic analysis of dorsoventral pattern formation in the zebrafish: requirement of a BMP-like ventralizing activity and its dorsal repressor. Genes Dev 1996;10:2452–2461.
28. Dale L, Wardle FC. A gradient of BMP activity specifies dorsal-ventral fates in early Xenopus embryos. Semin Cell Dev Biol 1999;10:319–326.
29. de Caestecker MP, Bottomley M, Bhattacharyya S, *et al.* The novel type I serine-threonine kinase receptor Alk8 binds TGF-beta in the presence of TGF-betaRII. Biochem Biophys Res Commun 2002;293:1556–1565.
30. Nakamura T, Gehrke AR, Lemberg J, Szymaszek J, Shubin NH. Digits and fin rays share common developmental histories. Nature 2016;537:225–228.
31. Chakkalakal SA, Zhang D, Culbert AL, *et al.* An Acvr1 R206H knock-in mouse has fibrodysplasia ossificans progressiva. J Bone Miner Res 2012;27:1746–1756.
32. Suzuki H, Ito Y, Shinohara M, *et al.* Gene targeting of the transcription factor Mohawk in rats causes heterotopic

ossification of Achilles tendon via failed tenogenesis. Proc Natl Acad Sci U S A 2016;113:7840–7845.
33. Culbert AL, Chakkalakal SA, Theosmy EG, *et al.* Alk2 regulates early chondrogenic fate in fibrodysplasia ossificans progressiva heterotopic endochondral ossification. Stem Cells 2014;32:1289–1300.
34. Hatsell SJ, Idone V, Wolken DMA, *et al.* ACVR1R206H receptor mutation causes fibrodysplasia ossificans progressiva by imparting responsiveness to activin A. Sci Transl Med 2015;7:303ra137.
35. Hino K, Ikeya M, Horigome K, *et al.* Neofunction of ACVR1 in fibrodysplasia ossificans progressiva. Proc Natl Acad Sci USA 2015;112:15438–15443.
36. Solnica-Krezel L, Schier AF, Driever W. Efficient recovery of ENU-induced mutations from the zebrafish germline. Genetics 1994;136:1401–1420.
37. MacRae CA, Peterson RT. Zebrafish as tools for drug discovery. Nat Rev Drug Discov 2015;14:721–731.
38. Meeker ND, Trede NS. Immunology and zebrafish: spawning new models of human disease. Dev Comp Immunol 2008;32:745–757.
39. Kaplan FS, Pignolo RJ, Shore EM. Granting immunity to FOP and catching heterotopic ossification in the act. Semin Cell Dev Biol 2016;49:30–36.
40. Kan L, Liu Y, McGuire TL, *et al.* Dysregulation of local stem/progenitor cells as a common cellular mechanism for heterotopic ossification. Stem Cells 2009;27:150–156.
41. Kan L, Lounev VY, Pignolo RJ, *et al.* Substance P signaling mediates BMP-dependent heterotopic ossification. J Cell Biochem 2011;112:2759–2772.
42. Shimono K, Tung W-E, Macolino C, *et al.* Potent inhibition of heterotopic ossification by nuclear retinoic acid receptor-γ agonists. Nat Med 2011;17:454–460.
43. Haupt J, Deichsel A, Stange K, *et al.* ACVR1 p.Q207E causes classic fibrodysplasia ossificans progressiva and is functionally distinct from the engineered constitutively active ACVR1 p.Q207D variant. Hum Mol Genet 2014.

Address correspondence to:
Pamela C. Yelick, PhD
Division of Craniofacial and Molecular Genetics
Department of Orthodontics
Tufts University School of Dental Medicine
136 Harrison Avenue, M824
Boston, MA 02111

E-mail: pamela.yelick@tufts.edu